

RESEARCH

Open Access

Functional up-regulation of Na_v1.8 sodium channel in A β afferent fibers subjected to chronic peripheral inflammation

Mounir Belkouch^{1,2}, Marc-André Dansereau¹, Pascal Tétreault¹, Michael Biet¹, Nicolas Beaudet¹, Robert Dumaine¹, Ahmed Chraïbi^{1†}, Stéphane Mélik-Parsadaniantz^{2†} and Philippe Sarret^{1*†}

Abstract

Background: Functional alterations in the properties of A β afferent fibers may account for the increased pain sensitivity observed under peripheral chronic inflammation. Among the voltage-gated sodium channels involved in the pathophysiology of pain, Na_v1.8 has been shown to participate in the peripheral sensitization of nociceptors. However, to date, there is no evidence for a role of Na_v1.8 in controlling A β -fiber excitability following persistent inflammation.

Methods: Distribution and expression of Na_v1.8 in dorsal root ganglia and sciatic nerves were qualitatively or quantitatively assessed by immunohistochemical staining and by real time-polymerase chain reaction at different time points following complete Freund's adjuvant (CFA) administration. Using a whole-cell patch-clamp configuration, we further determined both total I_{Na} and TTX-R Na_v1.8 currents in large-soma dorsal root ganglia (DRG) neurons isolated from sham or CFA-treated rats. Finally, we analyzed the effects of amroxol, a Na_v1.8-preferring blocker on the electrophysiological properties of Na_v1.8 currents and on the mechanical sensitivity and inflammation of the hind paw in CFA-treated rats.

Results: Our findings revealed that Na_v1.8 is up-regulated in NF200-positive large sensory neurons and is subsequently anterogradely transported from the DRG cell bodies along the axons toward the periphery after CFA-induced inflammation. We also demonstrated that both total I_{Na} and Na_v1.8 peak current densities are enhanced in inflamed large myelinated A β -fiber neurons. Persistent inflammation leading to nociception also induced time-dependent changes in A β -fiber neuron excitability by shifting the voltage-dependent activation of Na_v1.8 in the hyperpolarizing direction, thus decreasing the current threshold for triggering action potentials. Finally, we found that amroxol significantly reduces the potentiation of Na_v1.8 currents in A β -fiber neurons observed following intraplantar CFA injection and concomitantly blocks CFA-induced mechanical allodynia, suggesting that Na_v1.8 regulation in A β -fibers contributes to inflammatory pain.

Conclusions: Collectively, these findings support a key role for Na_v1.8 in controlling the excitability of A β -fibers and its potential contribution to the development of mechanical allodynia under persistent inflammation.

Keywords: A β -fibers, Allodynia, Complete Freund's adjuvant, Electrophysiology, Sodium channel blocker

Background

The processing of sensory information from primary afferent neurons to the spinal dorsal horn may change significantly following tissue inflammation, ultimately leading to the development of chronic pain. Abnormal pain manifestations, such as allodynia, hyperalgesia, and

spontaneous pain episodes occurring in these pathological pain states, are believed to result, at least in part, from plasticity phenomena in the spinal sensory system [1,2]. Functional alterations in the properties of A β primary afferents may notably account for the increased pain sensitivity observed under peripheral chronic inflammation. Variations in neurotransmitter content and release, changes in membrane receptor function and trafficking, and regulation of ion channel expression and activity may indeed enhance the excitability of A β -fibers and thus contribute to

* Correspondence: Philippe.Sarret@USherbrooke.ca

†Equal contributors

¹Department of Physiology and Biophysics, Faculty of Medicine and Health Sciences, Université de Sherbrooke, 3001, 12th Avenue North, Sherbrooke, Quebec J1H 5N4, Canada

Full list of author information is available at the end of the article

the development of mechanical hypersensitivity following peripheral chronic inflammation [1-3].

There is now considerable evidence supporting the idea that hyperexcitability and spontaneous action potential firing mediated by voltage-gated sodium channels in peripheral sensory neurons play an important role in the pathophysiology of chronic pain [4,5]. Among them, the slow-inactivating tetrodotoxin-resistant (TTX-R) sodium channel, Na_v1.8, has been pointed as a key contributor in the development of painful sensations associated with chronic inflammation in peripheral tissues [4,6]. Accordingly, several inflammatory mediators acting through G protein-coupled receptors, including adenosine, serotonin, prostaglandins, and chemokines, have been shown to sensitize TTX-R sodium channels and therefore to increase sensory neuron excitability [7-10]. Furthermore, functional knockdown of Na_v1.8 in rodents and spinal or systemic administration of Na_v1.8 channel blockers attenuate nociceptive behaviors related to persistent inflammation [4,5,11,12]. Although the Na_v1.8 channel is localized predominantly in small/medium nociceptive C/Aδ-type dorsal root ganglia (DRG) neurons, Na_v1.8 is also expressed by large myelinated Aβ afferent fibers in both healthy and inflamed animals [13-25]. We therefore hypothesized that the changes in the biophysical and pharmacological properties of Na_v1.8 might modulate the excitability of large-diameter sensory neurons under chronic peripheral inflammation.

In the present study, we thus investigated both total I_{Na} and TTX-R Na_v1.8 currents in large-soma DRG neurons isolated from sham or complete Freund's adjuvant (CFA)-treated rats, a well-established animal model of chronic inflammatory pain. We further determined whether this persistent inflammation led to alterations in the expression and localization pattern of Na_v1.8 in Aβ afferent fibers and redistribution in peripheral axons. Finally, we also examined the effects of ambroxol [26], a Na_v1.8-preferring blocker, on the electrophysiological properties of Na_v1.8 currents and on the development of mechanical allodynia following intraplantar CFA injection.

Methods

Animals and chronic inflammation induction

Adult male Sprague–Dawley rats (200 to 225 g, Charles River, St. Constant, Québec, Canada) were housed two per cage in a climate-controlled room on a 12 h light/dark cycle with water and food available ad libitum. They were allowed at least 5 days to habituate to the housing facility prior to manipulation and 1 hour to habituate to the experimentation room before any behavioral study was performed. All experimental procedures were approved by the Animal Care and Use Committee of the Université de Sherbrooke, and were in accordance with the policies and directives of the Canadian Council on Animal Care and guidelines from the International Association for the Study of Pain.

CFA (Calbiochem, La Jolla, CA, USA) was prepared by complementing it with 7 mg/ml of *mycobacterium butyricum* (Difco Laboratories, Detroit, MI, USA) and emulsified 1:1 with saline 0.9%. Under light anesthesia with isoflurane, rats received an intraplantar injection of 100 μl (400 μg) of the freshly emulsified mixture into the left hind paw. Sham animals received an intraplantar injection of 100 μl of saline.

Drugs

On days 3, 8, and 14 post-CFA administration, every rat was given an intrathecal (i.t.) injection of ambroxol (0.1 mg/kg, Sigma-Aldrich), a Na_v1.8-preferring sodium channel blocker or vehicle (DMSO 6%), for a total of three injections per rat [27]. Ambroxol was delivered between the lumbar vertebrae L5 and L6 in a final volume of 25 μl to lightly anesthetized animals with a Hamilton syringe fitted to a 27^{1/2} gauge needle. The cumulative dose of ambroxol (0.3 mg/kg) was chosen based on previous literature reporting affinity, selectivity, and in vivo profiles of this compound [27-29]. Mechanical sensitivity and edema were then determined (see details below) 1 h after the last administration of the drug. I.t. injection of drug solutions and behavioral testing were conducted on the basis of a blind and randomized design, in which one experimenter took the charge of drug preparation, whereas another experimenter who was blind to drug administration, randomly divided rats into two groups and conducted the measurements of mechanical withdrawal threshold and paw volume. Cultured DRG neurons isolated from rats treated for 14 days with CFA were also incubated for 30 min with ambroxol, applied at two different concentrations (20 and 100 μM) before patch clamp recordings.

Mechanical sensitivity

The onset and progression of mechanical hypersensitivity over a 21-day period in this CFA model has been previously published elsewhere [30]. Mechanical sensitivity testing was done in all rats prior to collection of tissue samples at days 3, 8, and 14 post-CFA using an electronic von Frey device (Ugo Basile Dynamic Plantar Aesthesiometer, Stoelting, IL, USA). Briefly, a dull metal probe (0.5 mm diameter), placed underneath a mesh floor, was applied against the hind paw pad and triggered when the animals were standing firmly. The probe exerted a ramping pressure of 3.33 g/sec. The force required to elicit a withdrawal response was automatically recorded upon the withdrawal of the hind paw and taken as the index of mechanical nociceptive threshold; the cut-off was set to 50 g. Four stimulations were applied alternately on the CFA-injected ipsilateral and contralateral hind paws. Average ipsilateral and contralateral paw withdrawal thresholds were calculated for

each animal. Rats were acclimatized to the device for 3 days before testing. On the 14th day following CFA administration, a chronic inflammation-induced hypersensitivity state was observed.

Edema

The volume of the hind paw was determined with a plethysmometer (Stoelting (Panlab), IL, USA) in rats treated for 14 days with CFA as well as in sham animals. The inflexion point of the ankle joint was used as an anatomical reference. The water displacement following immersion of the animal's paw in the measuring tube, into a second communicating tube induces a change in the conductance between the two platinum electrodes. The Plethysmometer Control Unit detects the conductance changes and generates an output signal to the digital display indicating the volume displacement (0.01 ml resolution).

Quantitative Real-Time PCR (qRT-PCR)

For qRT-PCR analysis, lumbar ipsilateral DRG (L4 to L6) were harvested on day 14 post-CFA injection, 1 h after the behavioral measurement, and then quickly snap frozen in dry ice. Total RNA was extracted using RNeasy® Mini Kits (Qiagen GmbH, Hilden, Germany). Both RNA quantity and quality were analyzed with a NanoDrop® 1000 spectrophotometer (Thermo Fisher Scientific, Wilmington, DE, USA). Reverse transcription of the samples was performed with TaqMan® Reverse Transcription Kits (Applied Biosystems, Carlsbad, CA, USA) using 400 ng of total RNA as template. Real time reactions were processed in triplicate for every cDNA sample on a Rotor-Gene 3000 (Corbett Life Science, Kirkland, Québec, Canada) using TaqMan® Gene Expression Master Mix (Applied Biosystems). Na_v1.8 levels were normalized against the housekeeping gene GAPDH and analyzed by the relative standard curve method. DNA oligonucleotides and probes used in Taqman assay are listed in Additional file 1: Table S1. The probes were conjugated with fluorescent reporter dyes 6-FAM at the 5' end and the quencher dye Iowa Black FQ at the 3' end (Integrated DNA Technologies, Inc., Coralville, IA, USA).

Axonal transport of Na_v1.8 in the sciatic nerve and quantification

To visualize the intra-axonal transport of Na_v1.8, a single ligature was placed around the sciatic nerve proximal to the trifurcation on day 12. Briefly, the left sciatic nerve of sham or CFA-treated rats was exposed at the level of the upper thigh, and tightly ligated with a 4.0 silk suture under deep anesthesia. At 48 h post-ligation, on day 14, 3-mm-long sciatic nerve segments proximal to the ligature were then harvested and processed for histology, as described below. For the quantification, sciatic nerve sections of CFA-injected animals (n = 9) or sham animals

(n = 3) were successively photographed with the same camera parameters (Axio Vision; Carl Zeiss, Oberkochen, Germany). The accumulation of Na_v1.8-immunoreactivity was examined in the sciatic nerve in an area of 1 mm proximal to the ligation site. The same threshold in grey levels was applied to all sections and the percentage of labeling density per fixed area of the Na_v1.8-immunoreactivity was quantified with Image J (version 1.46r, NIH) and reported as arbitrary units.

Immunolocalization of Na_v1.8 in dorsal root ganglia and sciatic nerves

At 3, 8, and 14 days after CFA or sham injection, rats were deeply anesthetized with ketamine (87 mg/kg)/xylazine (13 mg/kg) administered intramuscularly and perfused transaortically with a freshly prepared solution of 4% paraformaldehyde (PFA) in 0.1 M phosphate buffer saline (PBS), pH 7.4. Ipsilateral lumbar L4-L6 DRGs were rapidly removed, cryoprotected overnight in 0.1 M PBS containing 30% sucrose at 4°C, and snap frozen in isopentane cooled at -40°C. Tissues were sectioned longitudinally at a thickness of 20 µm on a Leica CM1850 cryostat. The sections were then processed for indirect immunofluorescence labeling, as previously described [31]. Briefly, serial sections were treated for 30 min at room temperature in a blocking solution containing 2% normal goat serum (NGS) and 0.5% Triton X-100 in PBS, and incubated overnight at 4°C with a mixture of primary antibodies in PBS containing 0.05% Triton X-100 and 0.5% NGS. To detect Na_v1.8, sections were incubated with the rabbit polyclonal anti-Na_v1.8 antibody (1:200; Alomone Labs, Jerusalem, Israel) in PBS containing 0.05% Triton X-100 and 0.5% NGS. To identify Na_v1.8-expressing large sensory neurons, DRG sections were processed for double immunofluorescence labeling with the mouse monoclonal anti-neurofilament 200 (1:400; NF200-clone N52; Sigma, Oakville, ON, Canada). After extensive washing with PBS, bound primary antibodies were revealed by simultaneous incubation with goat anti-rabbit Alexa 488- and goat anti-mouse Alexa 594-conjugated secondary antibodies (1:500; both from Molecular Probes, Burlington, ON, Canada) for 60 min at room temperature. After rinsing, sections were mounted in anti-fade mounting medium for fluorescent microscopy. For specificity control, sections were incubated overnight with primary antiserum pre-adsorbed with the Na_v1.8 corresponding antigen. The absence of cross-reactivity of the secondary antibodies was also verified by omitting one or both primary antibodies during the overnight incubation. The same procedure was performed for preparing the ligated sciatic nerves on day 14.

Image acquisition and analysis

Labeled sections were examined under fluorescent illumination with a Leica DM-4000 automated research

microscope (Leica, Dollard-des-Ormeaux, QC, Canada) equipped with a Lumenera InfinityX-21 digital camera using Infinity Capture software (Lumenera Corporation, Ottawa, ON, Canada) or analyzed by confocal microscopy using an Olympus Fluoview 1000 (FV1000) laser-scanning IX81-ZDC inverted microscope (Olympus Canada, Markham, ON, Canada). For the quantitative analysis of the number of Na_v1.8-positive neurons, three immunofluorescence stained non-consecutive sections (90 μm apart from each other in the z axis) were imaged per ganglion. The data were collected from three animals at each time point (3, 8, and 14 days following CFA injections). Three age-matched sham rats were used as controls to set standard acquisition parameters (laser power, HV gain, offset). The threshold for negative cells was determined with MetaMorph (version 7.7 from Molecular Devices, LLC, Sunnyvale, CA, USA). All neurons showing a higher mean intensity than the baseline threshold were considered as Na_v1.8-positive cells. To quantify the proportion of Na_v1.8-positive cells within a defined subset of sensory neurons, we counted the number of positive neurons for Na_v1.8 detected in NF200-immunoreactive neuronal profiles.

Preparation of DRG neurons

Neurons were acutely dissociated from lumbar dorsal root ganglia of adult rats and maintained in a short-term primary culture to be used within a 20 h period, as previously described [32]. Briefly, L4-L6 DRGs isolated from sham and CFA-injected rats were freed from their adherent connective tissues. After washing with calcium-magnesium free PBS (pH 7.4), DRGs were incubated sequentially for 120 min in enzyme solutions containing collagenase A (1 mg/ml; Roche Diagnostics, Indianapolis, IN, USA) and then trypsin (0.25%; GIBCO, Burlington, ON, Canada). Subsequently, ganglia were mechanically dissociated into single cells by repeated trituration through a fine-polished Pasteur pipette in culture medium containing 1:1 Dulbecco's modified Eagle's medium (DMEM, Invitrogen) and Ham's F12 supplemented with 10% fetal bovine serum (GIBCO) and 1% penicillin (100 U/ml)/streptomycin (0.1 mg/ml). Isolated neurons were gently centrifuged (50 g for 3 min), plated onto poly-D-lysine/laminin-coated glass coverslips, and maintained at 37°C in a humidified 95% air/5% CO₂ incubator before they were used for *in vitro* patch-clamp electrophysiology and immunocytochemistry. The immunocytochemical detection of Na_v1.8- and NF200-positive cells was performed 48 h after plating to allow them sufficient time to adhere. Isolated DRG neurons were then fixed for 15 min with 4% PFA before they were processed for immunostaining as described above.

Electrophysiological measurements

Total sodium currents (I_{Na}) and TTX-R Na_v1.8 currents were recorded from single, large-soma DRG neurons

(Capacitance >70 pF) in the whole-cell patch-clamp configuration 14 to 20 h after plating, using an Axopatch 200 B amplifier (Molecular devices, Sunnyvale, CA, USA). No significant difference was found in the capacitance between any of the groups. Short-term culture provided cells with truncated (<10 μm) axonal processes that can be voltage clamped readily and reliably and minimized changes in electrical properties that can occur in long-term culture. All experiments were performed at room temperature (21 to 23°C).

The intracellular recording electrodes were fabricated from borosilicate glass capillary tubes (Warner Instrument, Hamden, CT USA), pulled using a two-step vertical micropipette puller P83 (Narishige, Japan) and heat-polished on a microforge (Narishige). For sodium current measurements, the pipette solution contained (in mM): 10 NaCl, 140 CsCl, 10 EGTA, 1 MgCl₂, 2 Na₂ATP, 10 HEPES; pH adjusted to 7.2 by CsOH. Osmolarity was adjusted to 300 mOsm/l with sucrose. Pipettes had a resistance of 2 to 4 MΩ when filled with the pipette solution. Capacity transients were cancelled using computer-controlled circuitry and series resistance was compensated (>85%) in all experiments. The external solution contained (in mM): 35 NaCl, 65 NMDG-Cl, 30 TEA-Cl, 0.1 CaCl₂, 0.1 CoCl₂, 5 MgCl₂, 10 HEPES, and 10 glucose (pH adjusted at 7.4 by NaOH and osmolarity adjusted to 300 mOsm/l). The TEA-Cl and CoCl₂ was used to inhibit endogenous K⁺ and Ca²⁺ currents, respectively. The sodium concentration was reduced to 35 mM in order to maintain an adequate clamp of the current. After formation of a tight seal, membrane resistance and capacitance were determined.

Total sodium currents were recorded with a 5-ms prepulse to -120 mV followed by a 500-ms test pulse. TTX-R Na_v1.8 currents were isolated by prepulse inactivation as described earlier [33,34]. Briefly, standard current-voltage (I-V) families were constructed using a holding potential of -120 mV with 500-msec prepulses to -50 mV before each depolarization to inactivate the fast TTX-sensitive (TTX-S) currents. Thus, standard I-V curves were obtained by the application of a series of test pulses to voltages that ranged from -70 to +40 mV in 10 mV increments after the prepulse inactivation protocol. The voltage dependence of steady-state inactivation was measured by applying a double-pulse protocol consisting of a 500-ms conditioning potential (-120 to -10 mV, 5 mV increments) followed by a fixed test pulse (-10 mV, 50-ms). The current amplitude (I) was normalized to the maximum control current amplitude (I_{max}). For action potential measurements, the potassium channel blocker CsCl was replaced by an equimolar concentration of K-aspartate in the intracellular solution. The external solution contained (in mM): 145 NaCl, 1.8 CaCl₂, 5.4 KCl, 2 MgCl₂, 20 HEPES, and 10

glucose (pH adjusted at 7.4 by NaOH and osmolarity adjusted to 300 mOsm/l). Following formation of a giga-seal, a series of 1 ms current steps in 0.1 nA increments was injected into the cell under current-clamp mode. The threshold current needed to trigger an action potential was compared between control and CFA-treated animals in the presence or absence of TTX.

Data analysis

The peak inward current values at each potential were plotted to generate I-V curves. Conductance (G) was determined as $I/(V_m - V_{rev})$, where I is the current, V_m is the potential at which current is evoked, and V_{rev} is the reversal potential of the current. Activation was fitted with the following Boltzman equation: $G = G_{max}/[1 + \exp[(V_{1/2} - V_m)/k]]$, where V_m is the test pulse voltage potential at which current is evoked, G_{max} is the calculated maximal conductance, $V_{1/2}$ is the potential of half activation or inactivation, and k is the slope factor. The normalized curves were fitted using a Boltzmann distribution equation: $I = I_{max}/[1 + \exp[(V_{1/2} - V_m)/k]]$, where I_{max} is the peak sodium current elicited after the most hyperpolarized prepulse, V_m is the pre-conditioning pulse potential, $V_{1/2}$ is the half maximal sodium current, and k is the slope factor. Sodium currents were recorded using a Digidata 1440 A data acquisition system (Molecular devices) digitized at 10 kHz, low-pass filtered at 2 kHz and captured using pClamp software (v10.2, Molecular devices). For current density measurements, the currents were divided by the cell capacitance as read from the amplifier. The offset potential was zeroed before patching the cells and leakage current was digitally subtracted online using hyperpolarizing potentials, applied after the test pulse. Curves were plotted and fitted using Origin software (OriginLab Corporation, Northampton, MA, USA).

Statistics

Calculations and statistical analyses were performed using Prism 6.0 (Graph Pad Software, San Diego, CA, USA). All data are given as mean \pm standard error of the mean (SEM). *P* values <0.05 were considered statistically significant. Von Frey, plethysmometer, and electrophysiological data as well as the immunostaining data comparing the proportion of $Na_v1.8$ -positive neurons in CFA-treated rats to sham animals were analyzed using one-way ANOVA followed by a Holm-Sidak post hoc test. qRT-PCR and $Na_v1.8$ immunolabeling intensity in the sciatic nerve were compared between sham and CFA-treated rats with unpaired Student's *t*-test.

Results

Changes in $Na_v1.8$ channel distribution and expression during development of chronic inflammation

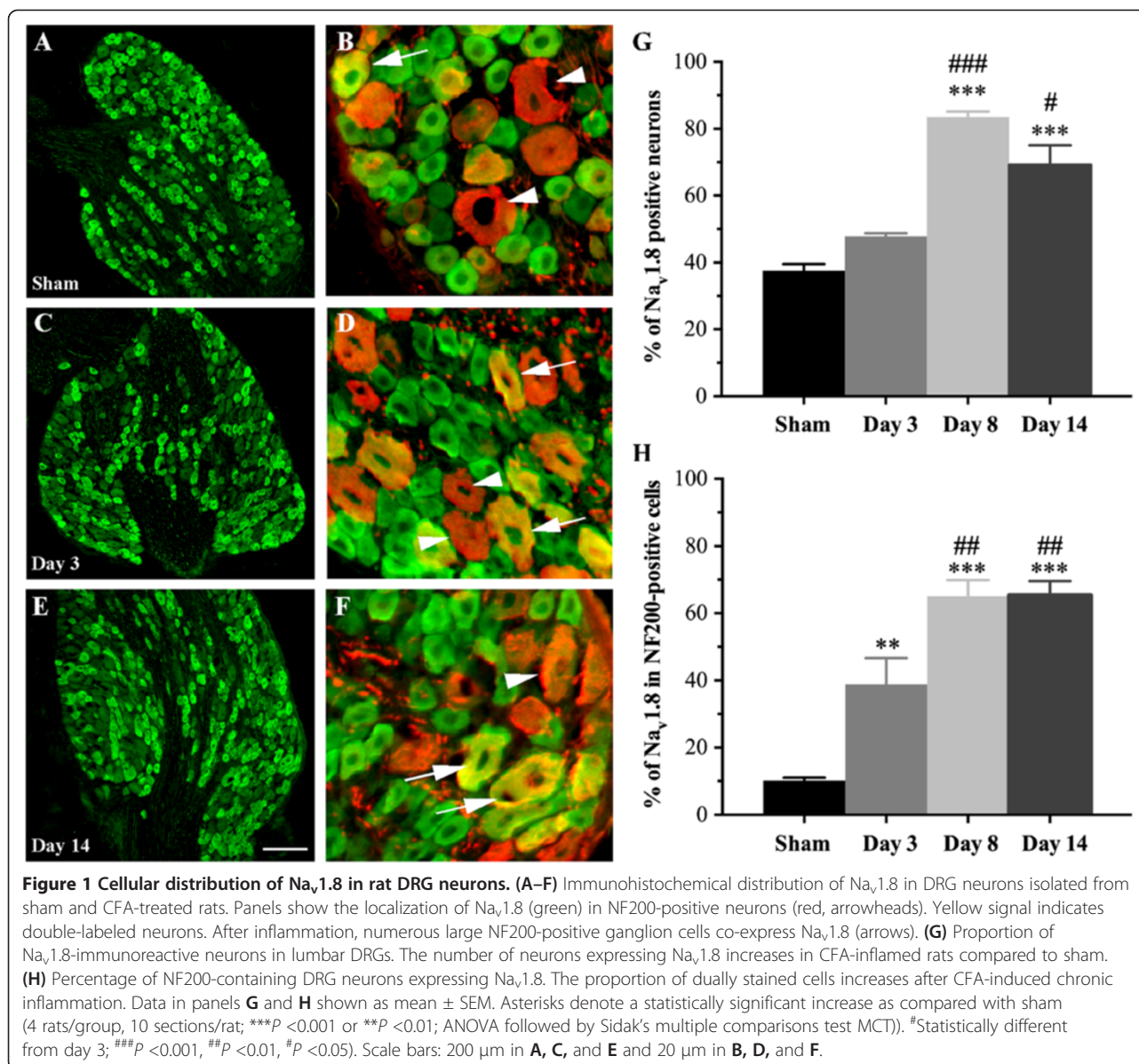
Pharmacological and physiological studies suggest that proinflammatory cytokines involved in the generation of

pain sensitize primary afferent nociceptors by increasing voltage-gated Na^+ currents [4,35]. In the present study, we therefore evaluated whether the cellular distribution of $Na_v1.8$ within DRG neurons was altered by hind paw injection of CFA. To do so, we first determined, by immunohistochemical staining, the proportion of $Na_v1.8$ -expressing neurons in DRG tissues of sham and CFA-inflamed rats (Figure 1). Strong $Na_v1.8$ labeling was evident in small to large ganglion cell bodies, this staining being completely prevented by preincubation with the cognate peptide (data not shown). Quantitative analysis revealed that approximately 35% of sensory neurons of all sizes displayed $Na_v1.8$ immunoreactivity in sham animals (Figure 1A,G). The number of $Na_v1.8$ -positive cells significantly increased on days 8 ($84\% \pm 1.6$; $***P < 0.001$; Figure 1G) and 14 ($69\% \pm 6$; $***P < 0.001$; Figure 1E,G) following intraplantar administration of CFA, compared to sham ($38\% \pm 2$; Figure 1A,G). A time-related effect was also seen when comparing days 8 ($###P < 0.001$) and 14 ($#P < 0.05$) to the early day 3 (Figure 1G).

To identify the subpopulation of large sensory neurons expressing $Na_v1.8$, tissue sections of DRGs were then processed for double-labeling immunohistochemistry combining $Na_v1.8$ antibodies with the high molecular weight (200 kDa) neurofilament protein NF200, a myelinated A-fiber ganglion cell marker. We found that about 10% of NF200-immunopositive cells expressed $Na_v1.8$ -like immunoreactivity in sham rats (Figure 1B, H). In contrast, NF200 co-localized extensively with $Na_v1.8$ during the persistent inflammatory state. Specifically, $39\% (\pm 8; **P < 0.01)$, $65\% (\pm 5; ***P < 0.001)$, and $65\% (\pm 4; ***P < 0.001)$ of NF200-positive ganglion cells exhibited $Na_v1.8$ -like staining at days 3, 8, and 14 after CFA injection, respectively (Figure 1D,E,H). Secondly, there were also significant differences between days after intraplantar CFA injection (Figure 1H). This increase in $Na_v1.8$ immunolabeling was accompanied by marked changes in its mRNA expression (Figure 2A). Compared to sham rats, high levels of $Na_v1.8$ transcripts were expressed in ipsilateral lumbar DRGs isolated 14 days post-CFA.

Intra-axonal transport of $Na_v1.8$ channels increases under persistent inflammation

We next examined if the gradual increase of the ipsilateral $Na_v1.8$ immunofluorescence and mRNA expression in DRG cell bodies observed after CFA-induced inflammation was followed by axonal protein trafficking toward sensory afferent terminals in peripheral tissues. To this end, the sciatic nerve was ligated for 2 days to verify the accumulation of transported $Na_v1.8$ at the ligation site. In sham animals, we found, using immunofluorescence staining, that $Na_v1.8$ was accumulating in the portion of the ligated sciatic nerve that was proximal to the



lumbar DRG (Figure 2B). This indicates that Na_v1.8 was anterogradely transported along the sciatic nerve to reach the peripheral terminals. No accumulation of Na_v1.8 was detected on the distal site and on the non-ligated contralateral side (not shown). More importantly, we found an increase in Na_v1.8-like immunoreactivity in the sciatic nerve at the proximal side, 14 days after CFA injection, compared to sham (**P* < 0.05; Figure 2C,D). These results thus suggest that newly synthesized Na_v1.8 proteins can be redistributed to peripheral afferent terminals after chronic tissue inflammation. Alternatively, the accumulation of Na_v1.8 channels at the ligation site may rely on mRNA axonal transport and local protein synthesis.

CFA-induced modulation of total I_{Na} currents in large-diameter sensory neurons

To determine if the changes in Na_v1.8 expression altered the total sodium current (I_{Na}) during development of chronic inflammation, we first measured the density of I_{Na} using a whole-cell configuration of the patch-clamp technique and characterized its kinetic properties in both normal and inflamed large sensory neurons. Representative recordings of total I_{Na} currents from large-soma rat DRG neurons (Capacitance >70 pF) are shown in Figure 3A. A series of depolarizing voltage commands from -80 to +40 mV were applied to activate all sodium channels in the cells. Maximum I_{Na} density increased at day 3 (-122.1 ± 4.9 pA/pF; ****P* < 0.001), day 8 (-112.8 ±

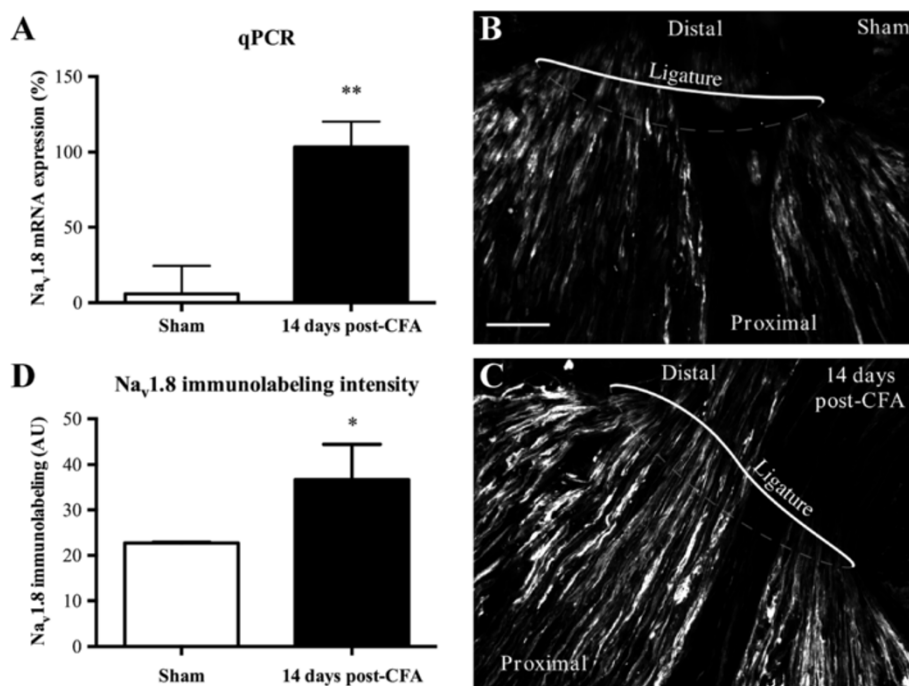


Figure 2 Changes in the expression and distribution of Na_v1.8 associated with CFA-induced inflammation in rats. **(A)** Na_v1.8 mRNA levels of the ipsilateral hind paw are determined by qRT-PCR for sham animals and 14 days following CFA injection. Data are expressed as mean ± SEM (6–8 rats/group). ***P* < 0.01, CFA alone vs. sham (unpaired Student's *t*-test). **(B, C)** Immunohistochemical staining of Na_v1.8 channels in the rat sciatic nerve proximal to the lesion site 48 h after ligation. The ligature was placed around the sciatic nerve proximal to the trifurcation on day 12 post-CFA. Scale bar: 100 μm. **(D)** Accumulation of Na_v1.8-like immunoreactivity is significantly increased in 14 day post-CFA rats compared to sham animals (**P* < 0.05; unpaired Student's *t*-test).

5.2 pA/pF; **P* < 0.05), and day 14 (−135.4 ± 4.1 pA/pF; ****P* < 0.001) in DRG neurons as CFA-induced inflammation developed, compared to sham cells (−90.7 ± 4.6 pA/pF) (Figure 3B,C; Additional file 2: Table S2). I_{Na} density was substantially higher on day 14 post-CFA, when compared to day 8 (**P* < 0.05). We next examined the voltage-dependence of activation of I_{Na} in CFA-treated and sham large DRG neurons. CFA treatment shifted the half-activation potential ($V_{1/2act}$) to a more negative potential in large-soma neurons isolated from rats treated for 8 days with CFA (−39.7 ± 1.6 mV; ***P* < 0.01) compared to sham neurons (−32.7 ± 0.8 mV), but had no significant effects in animals treated for 3 or 14 days (Figure 3D; Additional file 2: Table S2). These results therefore suggest that CFA enhanced or induced expression of new sodium channels in large DRG neurons. We next sought to determine if a change in the contribution of Na_v1.8 could be involved.

CFA increases Na_v1.8 currents in large-diameter sensory neurons

Dual immunostaining revealed that Na_v1.8 and NF200 immunoreactivities co-localized extensively over large-sized sensory neurons in acutely dissociated DRG cell cultures isolated from CFA-treated rats (Figure 4A). We

then tested if some of the changes in the biophysical properties of total I_{Na} correlated with an enhanced expression of Na_v1.8 in acutely dissociated lumbar NF200-positive sensory neurons (Capacitance >70 pF). In order to isolate the contribution of the TTX-R Na_v1.8 current from TTX-S sodium channels, we used a 500 ms inactivation prepulse to −50 mV. This protocol ensured that fast inactivating TTX-S channels did not contribute to I_{Na} measurements during the test pulse and biophysically isolate the more slowly inactivating TTX-R currents [33,34,36]. Furthermore, in this set of experiments, the membrane potential was held at −70 mV to inhibit the potential contribution of Na_v1.9 channels, thus leaving solely the Na_v1.8 current to be measured [37,38]. The resulting Na_v1.8 currents were elicited by applying series of 100 ms test pulses between −70 and +40 mV in 10 mV increments (Figure 4B).

Representative recordings of Na_v1.8 currents from both sham and inflamed large sensory neurons are shown in Figure 4B. Consistent with our immunostaining experiments, we found that CFA significantly increased Na_v1.8 current density compared to sham DRG neurons. I-V analysis revealed that CFA significantly increased the average maximum current density at days 3 (−63.7 ± 6.0 pA/pF; **P* < 0.05), 8 (−72.6 ± 2.9 pA/pF;

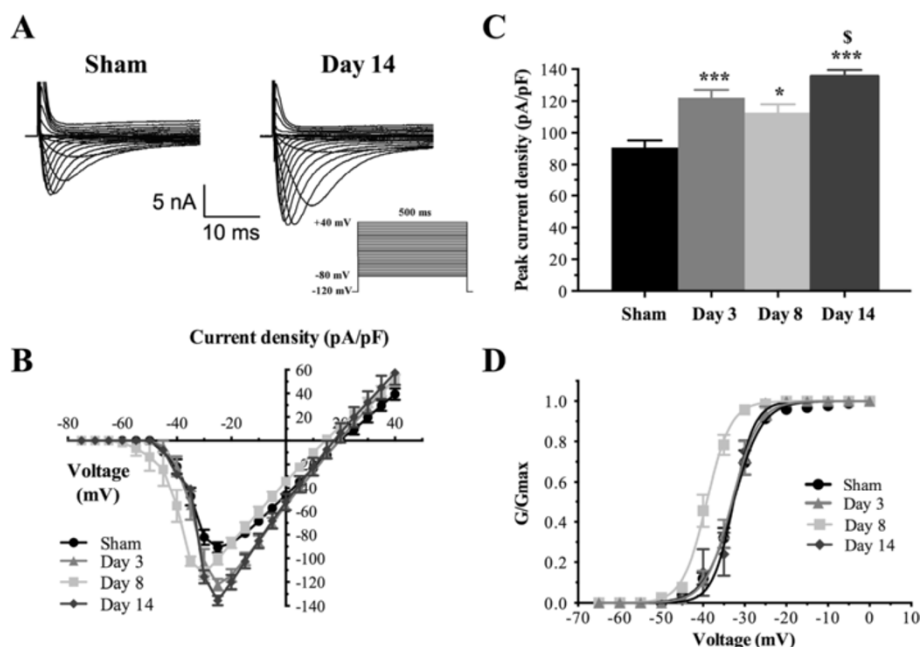


Figure 3 Total I_{Na} currents in large sensory neurons following exposure to CFA. **(A)** Whole-cell voltage-clamp current traces of I_{Na} are recorded from sham and CFA large-soma DRG neurons. Total currents were elicited by a series of 500-ms test pulses ranging from -80 to $+40$ mV in 5 mV steps. **(B)** I-V curves of total I_{Na} currents obtained from large-soma rat DRG neurons (Capacitance >70 pF). Maximum peak currents are observed at -25 mV in all groups with the exception of day 8 post-inflammation (-30 mV). **(C)** Histogram showing that the development of chronic inflammation induced by CFA intraplantar injection (days 3, 8, and 14 post-CFA) increases total I_{Na} peak currents. Data shown as mean \pm SEM (* $P < 0.05$, *** $P < 0.001$ vs. sham; $^S P < 0.05$ vs. day 8; ANOVA followed by Sidak's MCT; $n = 8-11$). **(D)** Voltage-dependent activation of total I_{Na} currents in large sensory neurons from inflamed rats. At day 8, CFA shifts the activation curve in a hyperpolarizing direction ($V_{1/2act} = -39.7 \pm 1.6$ mV for inflamed rats vs. -32.7 ± 0.8 mV for sham group; ** $P < 0.01$). Half-activation and half-inactivation potentials and slope factors are summarized in Additional file 2: Table S2.

*** $P < 0.001$), and 14 (-108.1 ± 1.5 pA/pF; *** $P < 0.001$) compared to sham DRG neurons (-49.6 ± 2.4 pA/pF) (Figure 4C,D). Interestingly, maximum current density at day 14 increased by more than 30% at day 14 compared to days 3 (SSS $P < 0.001$) and 8 (### $P < 0.001$) (Figure 4D; Additional file 3: Table S3).

Because $Na_v1.8$ channel kinetics differs from TTX-S channels it may influence the threshold for triggering action potentials, modulate the transmission of the neuronal electrical impulse and, as a consequence, influence nociception. We therefore determined if the development of chronic inflammation altered the voltage-dependence of activation and inactivation (availability) of $Na_v1.8$ currents. Our results show that CFA significantly hyperpolarized the midpoint of activation ($V_{1/2act}$) in large neurons from ipsilateral DRG after 14 days (-20.25 ± 0.6 mV) compared to sham neurons (-8.79 ± 1.01 mV; *** $P < 0.001$). Surprisingly, no shift in the activation curve was observed at days 3 (-9.3 ± 0.23 mV, $n = 6$; SSS $P < 0.001$) and 8 (-12.26 ± 1.01 mV, $n = 7$; ### $P < 0.001$) after CFA injection (Figure 4E, Additional file 3: Table S3).

CFA administration shifted the availability of $Na_v1.8$ channels (steady-state inactivation) in the hyperpolarizing direction at all time-points (Figure 4F) with half-

inactivation potentials ($V_{1/2inact}$) of -39.9 ± 1.34 mV (** $P < 0.01$), -38.4 ± 1.1 mV (* $P < 0.05$), and -56.3 ± 1.3 mV (*** $P < 0.001$) at days 3, 8, and 14, respectively, compared to control conditions (-33.6 ± 0.3 mV). Significant differences in $V_{1/2inact}$ were also observed between day 14 and days 3 (SSS $P < 0.001$) and 8 (### $P < 0.001$). Slope factors, k_{act} and k_{inact} , remained unchanged between sham and CFA-treated groups (Additional file 3: Table S3). Despite a significant shift in $Na_v1.8$ steady-state inactivation induced by CFA, examination of Figure 4F reveals that the loss of channel availability will be in order of 20% for a resting membrane potential around -70 mV. These results indicate that the drastic augmentation of 120% from -49.6 ± 2.4 pA/pF to -108.1 ± 1.5 pA/pF (Figure 4C,D) in $Na_v1.8$ current density is not due to changes in the availability of the channels but more likely result from enhanced expression of $Na_v1.8$ channels that largely compensate for the loss of channels to inactivation, thus confirming the qPCR and immunostaining data.

CFA increases excitability in large-diameter sensory neurons

The voltage dependence of activation of I_{Na} is known to determine the voltage threshold for triggering action

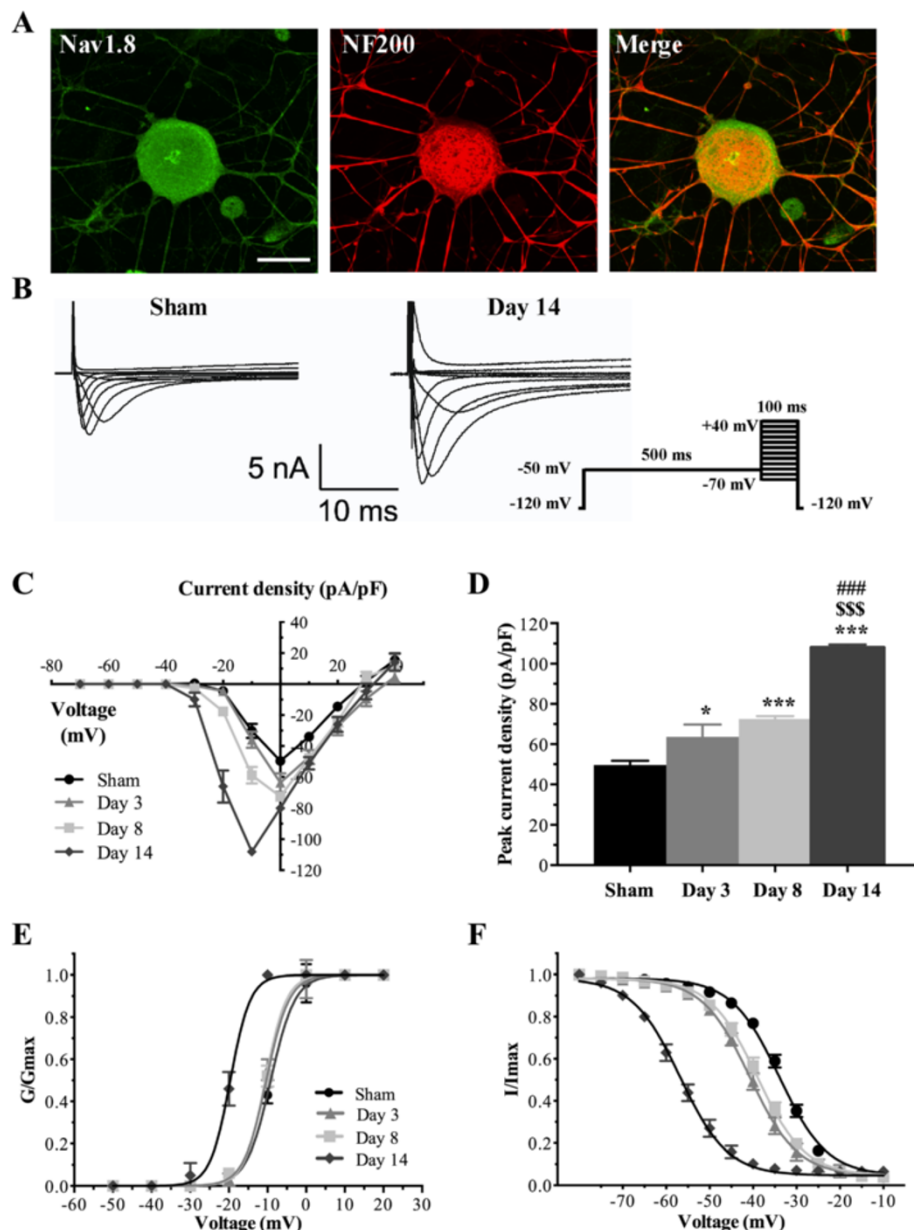


Figure 4 $\text{Na}_v1.8$ currents are enhanced in large-sized DRG neurons from inflamed rats. **(A)** Immunofluorescence staining of $\text{Na}_v1.8$ (green) and NF200 (red) on acutely dissociated primary afferent neurons, 14 days post-CFA. Merge images show dually labeled large-sized sensory neurons (yellow). **(B)** Isolation of TTX-resistant $\text{Na}_v1.8$ currents in large-sized sensory neurons from sham and inflamed rats. $\text{Na}_v1.8$ currents are significantly increased post-CFA. Representative I-V curves of currents are determined using the pulse protocol indicated in the inset. **(C)** I-V curves of $\text{Na}_v1.8$ currents obtained from large-soma DRG neurons. The peak maximum current is observed at 0 mV in all groups, with the exception of day 14 (-10 mV). **(D)** Peak $\text{Na}_v1.8$ current densities are significantly increased at days 3, 8, and 14 post-CFA injection ($***P < 0.001$ $*P < 0.05$ vs. sham; $^{$$$}P < 0.001$ vs. day 3; $^{###}P < 0.001$ vs. day 8; ANOVA followed by Sidak's MCT; $n = 6-13$). **(E, F)** Kinetic properties of $\text{Na}_v1.8$ currents in large-sized sensory neurons. CFA treatment induces a leftward shift of the activation **(E)** and inactivation **(F)** curves of $\text{Na}_v1.8$ current. Half-activation and half-inactivation potentials and slope factors are summarized in Additional file 3: Table S3.

potential in excitable cells. Our observation of a negative shift in the mid-activation potential of I_{Na} (Figure 4) suggests that the threshold potential for triggering an action potential is closer to the resting membrane potential and therefore renders CFA-treated DRG neurons more readily excitable. To test this hypothesis, we

measured the current threshold (I_{Th}) needed to trigger an action potential under current clamps in large sensory neurons isolated from sham or CFA-treated rats. Figure 5 shows that CFA significantly reduced I_{Th} from 0.26 ± 0.01 nA in sham cells to 0.17 ± 0.01 nA in CFA-treated large sensory neurons ($***P < 0.001$). To test for a

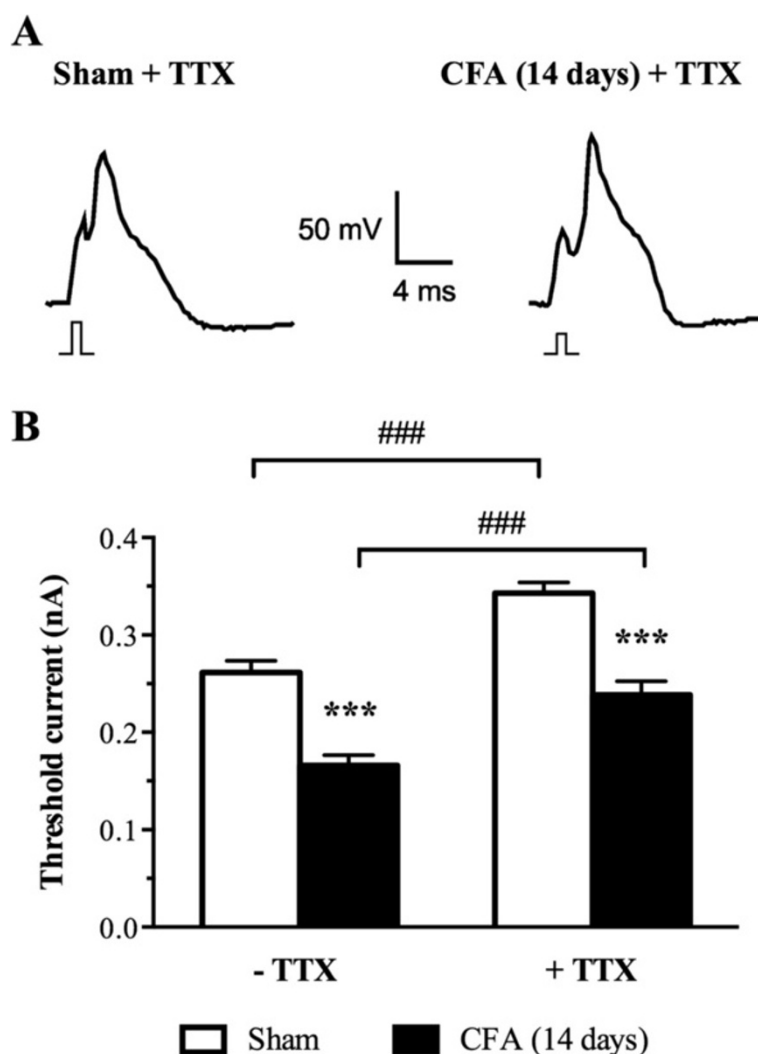


Figure 5 CFA increases excitability in large sensory neurons. (A) Representative recordings of DRG action potentials (AP) from sham and CFA-treated rats in the presence of 100 nM of tetrodotoxin (TTX). APs were triggered by a 1 ms current stimulus. The minimal (threshold) current amplitude needed to trigger APs was smaller in neurons from CFA-treated animals as illustrated by the smaller amplitude stimulus shown under each action potential. (B) Average threshold currents in sham and CFA conditions. CFA significantly decreased the amplitude of the current needed to trigger an action potential in neuronal cells exposed or not to 100 nM of TTX. Data shown as mean \pm SEM (*** P < 0.001, CFA vs. sham; ### P < 0.001, -TTX vs. + TTX ANOVA followed by Sidak's MCT; n = 14–22 from 3 rats in each condition).

specific contribution of TTX-R channels, we applied TTX in concentrations known to completely block TTX-S channels. Following application of 100 nM TTX, the action potential threshold was increased to 0.24 ± 0.01 nA and 0.34 ± 0.01 nA in CFA- and sham-treated neurons, respectively (Figure 5A,B). As expected, from the blockade of TTX-sensitive current, application of TTX increased the current needed to trigger an action potential by 31% and 42% in sham- and CFA-treated neurons, respectively. However, the changes in I_{Th} between CFA- and sham-treated cells slightly decreased from 35% in control to 30% upon application of TTX. These results therefore indicate that the major changes in I_{Th} are due to a contribution of TTX-R channels with

a smaller contribution of 5% coming from TTX-S and therefore reinforce the idea that inflammation increases large sensory neuron excitability by recruiting $Na_v1.8$ channel.

Ambroxol blocks CFA-induced potentiation of $Na_v1.8$ currents in large-diameter sensory neurons

To further confirm a contribution of $Na_v1.8$ to I_{Na} during chronic inflammation, we measured the sodium current in isolated large sensory neurons from CFA-injected rats following application of ambroxol, a preferring blocker of $Na_v1.8$. In agreement with our previous results, I-V analysis revealed that the increase in I_{Na} was considerably reduced following acute application of

ambroxol on neurons 14 days post-CFA (Figure 6). The average maximum current amplitude was decreased by 90% in inflamed large sensory neurons, following 30 min pre-incubation with 20 μM ambroxol (-10.7 ± 3.7 pA/pF

vs. -108.1 ± 1.5 pA/pF; $^{###}P < 0.001$) (Figure 6A,B). At the highest concentration tested (100 μM), the $\text{Na}_v1.8$ -preferring sodium channel blocker completely prevented the increase in peak current density induced by CFA (-1.5 ± 1.4 pA/pF vs. -108.1 ± 1.5 pA/pF; $^{###}P < 0.001$) (Figure 6A,B).

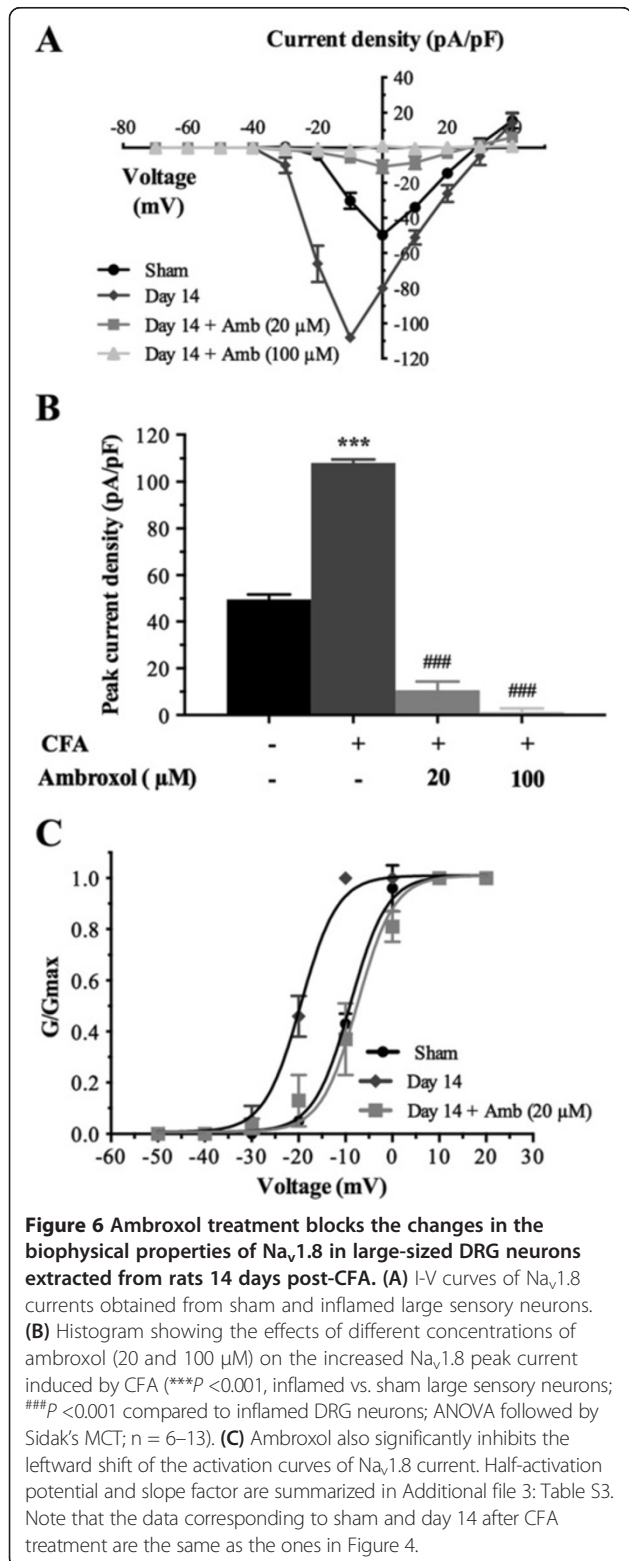
Our results also showed that ambroxol (20 μM) significantly blocked the hyperpolarizing shift in the activation curve of I_{Na} observed in response to CFA (Figure 6C). The half-activation potential ($V_{1/2\text{act}}$) was shifted to -8.52 ± 3.39 mV from that of CFA control condition (-20.25 ± 0.63 mV) after 20 μM ambroxol treatment ($^{###}P < 0.001$; Additional file 3: Table S3), thus reinforcing the notion that enhanced expression of $\text{Na}_v1.8$ increases the excitability of inflamed neurons.

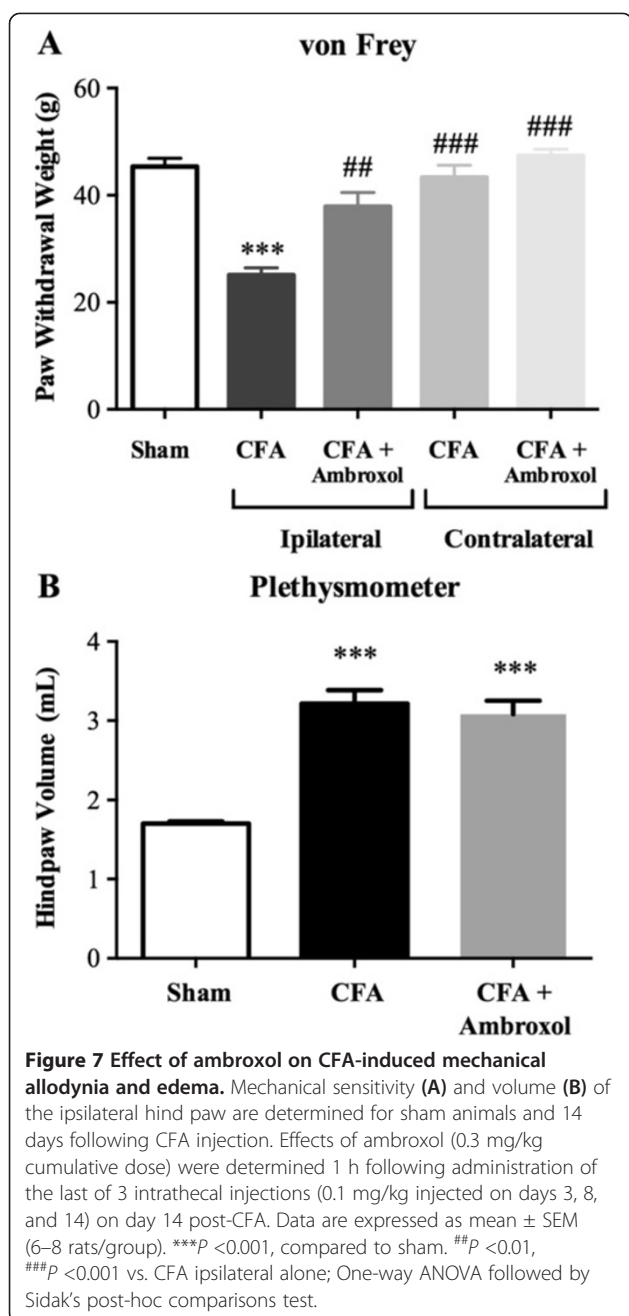
Inhibition of $\text{Na}_v1.8$ channel function by ambroxol

We then determined the ability of i.t. injections of ambroxol, a $\text{Na}_v1.8$ -preferring Na^+ channel blocker, to block the signs of nociception induced 14 days post-CFA. As shown in Figure 7A, CFA-treated rats exhibited paw withdrawals at reduced mechanical forces ($25 \text{ g} \pm 1.4$) compared to sham animals ($45 \text{ g} \pm 1.6$; $^{***}P < 0.001$), consistent with the development of mechanical hypersensitivity. In addition, CFA injection caused a marked increase in paw volume indicative of edema development, compared to shams ($3.2 \text{ ml} \pm 0.2$ vs. $1.7 \text{ ml} \pm 0.1$, respectively; $^{***}P < 0.001$; Figure 7B). Interestingly, i.t. ambroxol (0.1 mg/kg acute dose, 0.3 mg/kg cumulative dose) reduced mechanical allodynia by 63% in the CFA model of inflammatory pain ($^{##}P < 0.01$; Figure 7A). Additionally, ambroxol had no effect on paw withdrawal threshold of the contralateral non-inflamed paw, revealing specific anti-allodynic effects of the drug (Figure 7A). Furthermore, $\text{Na}_v1.8$ channel blockade by i.t. ambroxol did not modify the inflammation-induced paw swelling (Figure 7B).

Discussion

Voltage-gated sodium channels play a fundamental role in pain sensation under both physiological and pathological conditions [4,5]. Among them, $\text{Na}_v1.8$ has been shown to regulate sensory neuron excitability and thus to participate in the peripheral sensitization associated with the development of chronic pain [4,6]. Our findings herein revealed that $\text{Na}_v1.8$ is up-regulated in large myelinated A β -fiber neurons and is subsequently anterogradely transported from the DRG cell bodies along the axons toward the periphery after CFA-induced inflammation. We also demonstrated that the development of peripheral chronic inflammation was associated with both enhanced I_{Na} and $\text{Na}_v1.8$ current densities in NF200-positive A β -fiber neurons. Persistent inflammation further leads to time-dependent changes in A β -fiber





neuron excitability by shifting the voltage-dependent activation and steady-state inactivation curves of $Na_v1.8$ in the hyperpolarizing direction. In good agreement, we also found, using a current-clamp mode, that CFA-induced persistent inflammation enhances the excitability of $A\beta$ -fiber neurons. Finally, we found that ambroxol, a $Na_v1.8$ -preferring blocker, significantly reduces the potentiation of $Na_v1.8$ currents observed following intraplantar CFA injection and concomitantly blocks CFA-induced mechanical allodynia.

$Na_v1.8$ is up-regulated in $A\beta$ -fiber neurons under persistent inflammation

Functional alterations in the properties of $A\beta$ -fiber neurons may account for the increased pain sensitivity observed under peripheral chronic inflammation [2]. In particular, there is now considerable evidence that $A\beta$ afferent fiber neurons undergo significant changes in their electrical characteristics under chronic pain conditions [39–42]. We hypothesized here that the alteration in $Na_v1.8$ sodium channel expression, trafficking, and activity might substantially contribute to the enhanced excitability in injured $A\beta$ sensory neurons, thus allowing the development of mechanical allodynia. In the present study, we first examined the expression of $Na_v1.8$ in the defined subpopulation of NF200-positive neurons over a 14-day period following CFA injection. The immunocolocalization experiments revealed that $Na_v1.8$ is present in about 10% of NF200-positive large-soma DRG neurons from sham animals. These results are in accordance with previous studies reporting that 10% to 30% of large-diameter sensory neurons contain $Na_v1.8$ mRNA or are immunohistochemically labeled for the $Na_v1.8$ protein in sham animals [13–15,17–24,43,44]. Likewise, Shields et al. recently found, using $Na_v1.8$ -cre mice, that an even higher percentage of NF200-labeled neurons (around 40%) was $Na_v1.8$ -cre-positive [25].

Our results further demonstrated that $Na_v1.8$ expression increases dramatically in DRG neurons during inflammation, with 69% of all sensory neurons and 65% of NF200-positive ganglion cells exhibiting $Na_v1.8$ immunostaining 14 days post-CFA (compared to 35% and 10% in sham animals, respectively). This up-regulation of $Na_v1.8$ expression in DRG tissue has also been highlighted by others following short-term exposure to carrageenan or CFA (one to four days post-insult) [16,20,45,46]. The long-term effects of proinflammatory agents on $Na_v1.8$ expression was only observed 14 days after repeated intraplantar injections of PGE_2 or over a 28-day time course following intra-articular injection of CFA [47–49]. However, to date, relatively few studies have examined how these inflammatory conditions specifically affect the expression level of $Na_v1.8$ in injured $A\beta$ sensory neurons. Consistent with our findings, Coggeshall et al. have observed significant changes in $Na_v1.8$ expression (6-fold increase), reaching close to 60% of labeled myelinated axons in digital nerves 48 h post-CFA [50]. Altogether, these findings suggest that up-regulation of $Na_v1.8$ under peripheral chronic inflammation may be responsible for at least some of the changes in $A\beta$ -fibers.

Persistent peripheral inflammation increases the anterograde transport of $Na_v1.8$

Redistribution of voltage-gated channels along the peripheral axolemma has also been proposed to significantly influence nociceptor excitability and to be in part responsible

for the spontaneous ectopic discharges generated by damaged peripheral sensory nerves [4,5,51]. In this study, we thus asked whether Na_v1.8 was transported to injured peripheral terminals during chronic tissue inflammation. Our results revealed that Na_v1.8 immunoreactivity was increased in axons proximal to the site of injury in uninflamed rat sciatic nerve 48 h following ligation. More importantly, CFA-induced peripheral inflammation resulted in a significantly increased accumulation of Na_v1.8 immunostaining at the ligated site, compared to uninflamed nerves. These data thus indicate that non-physiological nociceptive afferent excitation induces intra-axonal anterograde trafficking of Na_v1.8 from DRG cell bodies to peripheral terminals. In support of these results, rats that received CFA into the upper lip/whisker pad were shown to exhibit an increase in Na_v1.8 immunoreactivity in the infraorbital nerve 48 hours and one week after CFA treatment, revealing transport of Na_v1.8 protein to the periphery [52].

Although the role of Na_v1.8 in the generation and maintenance of neuropathic pain is not completely defined and remains controversial, it has been found in several nerve injury-based rodent models of peripheral neuropathy that Na_v1.8 immunoreactivity strongly increased in the nerve proximal to the injury site [43,53,54]. Consistent with these findings, patients dealing with chronic neuropathic pain show increased Na_v1.8 channel accumulation at the sites of nerve injury [55-59]. The massive redistribution in Na_v1.8 immunoreactivity along the sciatic nerve might be attributed to the up-regulation of Na_v1.8 mRNA and protein levels within the cell bodies of sensory neurons, as we observed 14 days post-CFA administration. We might also hypothesize that Na_v1.8 mRNA redistribution in both myelinated and unmyelinated axons followed by local translation contributes to the increased immunoreactivity in the injured nerve, as previously reported in peripheral neuropathy [54,60]. These results reveal that the trafficking of Na_v1.8 to sensory nerve endings, such as those found in the skin, may play a significant role in the development and maintenance of peripheral sensitization and chronic pain states. This also suggests that blocking Na_v1.8 axonal transport may be effective for treating chronic neuropathic or inflammatory pain.

Peripheral inflammation enhances total I_{Na} and Na_v1.8 currents in Aβ-fiber neurons

Primary hyperalgesia is mainly due to sensitization of the peripheral terminals of nociceptors and is the consequence of an increase in their membrane excitability and/or a reduction in their action potential threshold. This alteration of the sensory transmission is typically triggered by pro-inflammatory mediators released by damaged tissues and infiltrating immune cells. Among these hyperalgesic agents, the prostaglandins PGE2 and

PGD2 and the chemokine CCL2, as well as adenosine, serotonin, and substance P were found to regulate current amplitude and conductance of TTX-R sodium channels on small- and medium-sized sensory neurons [7,9,10,37,61,62]. However, to date, very few studies have investigated the changes in voltage-sensitive sodium currents in experimental models of persistent inflammation, and all of them have focused only on small/medium-sized primary afferent neurons [20,46,63-65]. Since allodynia is believed to be mediated by large Aβ-fibers, we investigated here whether the induction of chronic peripheral inflammation by an intraplantar injection of CFA induced significant changes in the biophysical properties of sodium channels (notably Na_v1.8) in NF200-positive large Aβ-fiber neurons.

Our electrophysiological recordings performed in the whole-cell patch-clamp configuration revealed that both I_{Na} and Na_v1.8 peak current densities were larger in the CFA-injected group at all time-points (3, 8, and 14 days) after CFA injection than in the sham group. Accordingly, we also found under current-clamp experiments that CFA-induced persistent inflammation decreased the current threshold for action potential initiation, thus enhancing the excitability of Aβ-fiber neurons. Our data are consistent with previous studies performed on small sensory neurons demonstrating that short-term exposure (<5 days) to carrageenan or CFA treatment produced an increase of both TTX-R and TTX-S Na⁺ current amplitudes [20,46,63-65]. However, as opposed to those studies, we demonstrated here that the increased amplitude was accompanied by hyperpolarizing shifts in the voltage-dependence of activation and steady-state inactivation. These findings thus suggest that the voltage-dependent and kinetic properties of DRG sodium currents can depend either on the neuronal cell-type (small vs. large sensory neurons), on the type of inflammatory agents used (carrageenan, CFA), or on the time course of inflammation (short- or long-term exposure).

Finally, our results revealed that the gating properties of I_{Na} and Na_v1.8 sodium currents along with the up-regulation of Na_v1.8 expression in DRG tissue are differentially regulated over the time course of the CFA challenge. These differences can be explained in part by the evolution of the early inflammation state to a transient inflammation condition at day 8 post-CFA, and finally to signs of arthritis at later time points (14 days) [66]. Furthermore, we also found that peripheral inflammation produced a leftward shift in activation voltage-dependency for the total sodium current at day 8 without any shift in the voltage-dependence of activation of Na_v1.8. One possibility is that TTX-S currents account for the transient negative shift in activation voltage-dependency observed at day 8 post-CFA. Based on previous findings indicating that TTX-R Na_v1.9 sodium currents are up-regulated in large

sensory neurons in painful diabetic neuropathy [18], we might also hypothesize that this channel is possibly involved in the changes of voltage-dependent properties of I_{Na} in A β -fiber neurons, 8 days following induction of peripheral inflammation.

Ambroxol blocks CFA-induced mechanical allodynia and potentiation of $Na_v1.8$ currents in A β -fiber neurons

Several lines of behavioral evidence indicate that the $Na_v1.8$ channel is an important contributor to the development of the hypersensitivity state that underlies inflammatory pain [4,5,11,12]. Indeed, studies with $Na_v1.8$ -null mice, $Na_v1.8$ blockers, antisense technology, and short inhibitory RNA (siRNA)-mediated knockdown approaches have demonstrated that inhibition of $Na_v1.8$ reduces the mechanical, thermal, and visceral responses in animal models of inflammatory pain [13,48,63,67-76]. In the present study, we showed that mechanical allodynia was significantly reduced at 14 days post-CFA by repeated i.t. administration of ambroxol (0.3 mg/kg cumulative dose), a $Na_v1.8$ -preferring channel inhibitor. Accordingly, ambroxol was also effective in reversing CFA-induced $Na_v1.8$ current amplitudes and gating properties in A β -fiber neurons. These results are in accordance with previous studies demonstrating that ambroxol suppresses the nociceptive behaviors associated with the development of chronic painful conditions, including neuropathic and inflammation [27,29,77,78]. In good agreement with these findings, systemic or i.t. administration of $Na_v1.8$ selective blockers (e.g., A-803467) was found to be active in reducing various nociceptive symptoms and to potently inhibit evoked and spontaneous firing of dorsal horn wide dynamic range neurons in inflammatory and neuropathic pain models [28,70,74,79,80]. Collectively, our findings suggest an interesting paradigm by which enhanced expression of $Na_v1.8$ increases the amplitude of the action potentials and may promote a more rapid transmission of the electrical impulse and, by virtue of $Na_v1.8$ biophysical properties, decrease the threshold for triggering action potentials and therefore increase excitability in A β -fiber neurons and its contribution to the development of mechanical allodynia under persistent inflammation.

How can these changes in $Na_v1.8$ function in large diameter myelinated A β -fiber neurons drive pain?

It is widely accepted that sensitization of C- and δ -fibers can directly result in increased pain. However, it is less obvious to explain how the increase of $Na_v1.8$ function in myelinated A β -fibers, which normally convey low threshold touch, can fill some of the roles of C- and δ -fibers under persistent inflammation and lead to the recruitment of postsynaptic pain signaling pathways. Different mechanisms can be put forward to explain how A β afferent fibers might come to evoke tactile allodynia in

the event of persistent inflammation. Notably, it has been proposed that large myelinated tactile A β afferent fibers, which normally arborize in laminae III–V, may sprout dorsally into the superficial laminae of the spinal cord dorsal horn and gain access to second order nociceptive neurons [81-87]. Alternatively, we can consider the possibility that the thick A β afferent fibers are the principal driver of pain sensation (tactile allodynia). Both peripheral nerve injury and chronic peripheral inflammation are known to potentiate intrinsic oscillations in membrane potential and increase ectopic discharges in DRG neurons [88,89]. Here, we found that CFA induced overexpression of $Na_v1.8$ combined with a negative voltage shift in I_{Na} activation lowered the threshold for triggering action potentials. Therefore, one expects the enhanced oscillatory behavior to increase ectopic firing as the oscillations more frequently reach the action potential threshold. Crosstalk or ephapsis do not normally occur within the DRG, as each sensory neuron is isolated from the others [90,91]. However, chemically mediated cross-excitation in the DRG and transient cross-depolarization in neighboring cells were observed in 90% of neurons within the DRG following tetanic stimulation [90,92]. A similar mechanism may also explain the mechanical allodynia in our CFA model. As overexpression of $Na_v1.8$ enhances excitability and the probability of spontaneous action potentials in DRG neurons, cross-depolarizations sufficient to evoke ectopic firing in neighboring nociceptive neurons may induce mechanical allodynia. Such a mechanism is supported by evidence of cross-excitation between A- and C-fibers [93].

Additional files

Additional file 1: Table S1. DNA oligonucleotides and probes used in the qPCR assay.

Additional file 2: Table S2. Properties of I_{Na} currents in sham and inflamed large sensory neurons. $V_{1/2act}$ is the membrane potential for half-maximal channel activation. k_{act} represents the slope factor for activation. * $P < 0.05$, ** $P < 0.01$, and *** $P < 0.001$ indicate statistically significant differences with sham group. ^S $P < 0.05$ compared to large-sized DRG neurons extracted from rats 14 days post-CFA to day 8. Numbers in parentheses reflect numbers of recorded neurons.

Additional file 3: Table S3. Mean peak sodium current amplitude, activation, and steady-state inactivation characteristics of $Na_v1.8$ currents in sham and inflamed large sensory neurons. $V_{1/2act}$ and $V_{1/2inact}$ are the membrane potentials for half-maximal channel activation or inactivation, respectively. k_{act} and k_{inact} represent the slope factors for activation and inactivation. * $P < 0.05$, ** $P < 0.01$, and *** $P < 0.001$ indicate statistically significant differences with sham group. ^{SS} $P < 0.001$ and ^{##} $P < 0.001$ compared to large-sized DRG neurons extracted from rats 14 days post-CFA to days 3 and 8, respectively. Numbers in parentheses reflect numbers of recorded neurons. Ambroxol also significantly inhibits the leftward shift of the activation curves of $Na_v1.8$ current (^{###} $P < 0.001$ compared to CFA-treated neurons).

Abbreviations

CFA: Complete Freund's adjuvant; DRG: Dorsal root ganglia; I_{Na} : Total sodium current; I-V: Standard current-voltage; TTX-R: Tetrodotoxin-resistant; TTX-S: Tetrodotoxin-sensitive.

Competing interests

The authors declare that they have no competing interests.

Authors' contributions

MBe performed the electrophysiological and immunohistochemical experiments presented in this manuscript. MAD realized the in vivo behavioral studies as well as the quantitative real-time PCR experiments. PT was involved in the immunostaining studies. MBI performed the electrophysiological studies under current-clamp mode. PS conceptualized the project and wrote the manuscript. NB, AC, RD, and SMP participated in the design of the experiments and edited the manuscript. All authors read and approved the manuscript.

Authors' information

Ahmed Chraïbi, Stéphane Mélik-Parsadaniantz, and Philippe Sarret: co direction of the work.

Acknowledgements

The authors would like to thank Mr. Alexandre Parent for his assistance in the preparation of primary cultures of DRG neurons. This work is supported by a grant from the Canadian Institutes of Health Research awarded to PS and SMP. MBe, MAD, and PT are respectively supported by the Lavoisier, Sir Frederick Banting and Dr. Charles Best Canada, and Natural Sciences and Engineering Research Council Graduate Scholarships. PS is a recipient of the Canada Research Chair in Neurophysiopharmacology of Chronic Pain, director of the Sherbrooke's Neuroscience Centre, and member of the FRQS-funded Centre de Recherche Clinique Étienne Lebel.

Author details

¹Department of Physiology and Biophysics, Faculty of Medicine and Health Sciences, Université de Sherbrooke, 3001, 12th Avenue North, Sherbrooke, Quebec J1H 5N4, Canada. ²Pain Group, Centre de Recherche de l'Institut du Cerveau et de la Moelle Épinrière, Université Pierre et Marie Curie, INSERM-Unité Mixte de Recherche en Santé 975, CNRS-Unité Mixte de Recherche 7225, 75013 Paris, France.

Received: 25 November 2013 Accepted: 21 February 2014

Published: 7 March 2014

References

1. Todd AJ: Neuronal circuitry for pain processing in the dorsal horn. *Nat Rev Neurosci* 2010, **11**:823–836.
2. Kuner R: Central mechanisms of pathological pain. *Nat Med* 2010, **16**:1258–1266.
3. Ueda H: Molecular mechanisms of neuropathic pain-phenotypic switch and initiation mechanisms. *Pharmacol Ther* 2006, **109**:57–77.
4. Dib-Hajj SD, Cummins TR, Black JA, Waxman SG: Sodium channels in normal and pathological pain. *Annu Rev Neurosci* 2010, **33**:325–347.
5. Lampert A, O'Reilly AO, Reeh P, Leffler A: Sodium channelopathies and pain. *Pflugers Arch* 2010, **460**:249–263.
6. Amir R, Argoff CE, Bennett GJ, Cummins TR, Durieux ME, Gerner P, Gold MS, Porreca F, Strichartz GR: The role of sodium channels in chronic inflammatory and neuropathic pain. *J Pain* 2006, **7**:S1–S29.
7. Ebersberger A, Natura G, Eitner A, Halbhuber KJ, Rost R, Schaible HG: Effects of prostaglandin D(2) on tetrodotoxin-resistant Na(+) currents in DRG neurons of adult rat. *Pain* 2011, **152**(5):1114–1126.
8. Liu C, Li Q, Su Y, Bao L: Prostaglandin E2 promotes Nav1.8 trafficking via its intracellular RRR motif through the protein kinase A pathway. *Traffic* 2010, **11**:405–417.
9. Gold MS, Reichling DB, Shuster MJ, Levine JD: Hyperalgesic agents increase a tetrodotoxin-resistant Na⁺ current in nociceptors. *Proc Natl Acad Sci USA* 1996, **93**:1108–1112.
10. Belkouch M, Dansereau MA, Reaux-Le Goazigo A, Van Steenwinckel J, Beaudet N, Chraïbi A, Mélik-Parsadaniantz S, Sarret P: The chemokine CCL2 increases Nav1.8 sodium channel activity in primary sensory neurons through a Gbetagamma-dependent mechanism. *J Neurosci* 2011, **31**:18381–18390.
11. Matulenka MA, Scanio MJ, Kort ME: Voltage-gated sodium channel blockers for the treatment of chronic pain. *Curr Top Med Chem* 2009, **9**:362–376.
12. Priest BT: Future potential and status of selective sodium channel blockers for the treatment of pain. *Curr Opin Drug Discov Devel* 2009, **12**:682–692.
13. Abrahamsen B, Zhao J, Asante CO, Cendan CM, Marsh S, Martinez-Barbera JP, Nassar MA, Dickenson AH, Wood JN: The cell and molecular basis of mechanical, cold, and inflammatory pain. *Science* 2008, **321**:702–705.
14. Amaya F, Decosterd I, Samad TA, Plumpton C, Tate S, Mannion RJ, Costigan M, Woolf CJ: Diversity of expression of the sensory neuron-specific TTX-resistant voltage-gated sodium ion channels SNS and SNS2. *Mol Cell Neurosci* 2000, **15**:331–342.
15. Everill B, Cummins TR, Waxman SG, Kocsis JD: Sodium currents of large (Abeta-type) adult cutaneous afferent dorsal root ganglion neurons display rapid recovery from inactivation before and after axotomy. *Neuroscience* 2001, **106**:161–169.
16. Gould HJ 3rd, Gould TN, Paul D, England JD, Liu ZP, Reeb SC, Levinson SR: Development of inflammatory hypersensitivity and augmentation of sodium channels in rat dorsal root ganglia. *Brain Res* 1999, **824**:296–299.
17. Ho C, O'Leary ME: Single-cell analysis of sodium channel expression in dorsal root ganglion neurons. *Mol Cell Neurosci* 2011, **46**:159–166.
18. Hong S, Wiley JW: Altered expression and function of sodium channels in large DRG neurons and myelinated A-fibers in early diabetic neuropathy in the rat. *Biochem Biophys Res Commun* 2006, **339**:652–660.
19. Sangameswaran L, Delgado SG, Fish LM, Koch BD, Jakeman LB, Stewart GR, Sze P, Hunter JC, Eglén RM, Herman RC: Additions and corrections to structure and function of a novel voltage-gated, tetrodotoxin-resistant sodium channel specific to sensory neurons. *J Biol Chem* 1996, **271**:13292A–13292A.
20. Tanaka M, Cummins TR, Ishikawa K, Dib-Hajj SD, Black JA, Waxman SG: SNS Na⁺ channel expression increases in dorsal root ganglion neurons in the carrageenan inflammatory pain model. *Neuroreport* 1998, **9**:967–972.
21. Djouhri L, Fang X, Okuse K, Wood JN, Berry CM, Lawson SN: The TTX-resistant sodium channel Nav1.8 (SNS/PN3): expression and correlation with membrane properties in rat nociceptive primary afferent neurons. *J Physiol* 2003, **550**:739–752.
22. Renganathan M, Cummins TR, Hormuzdiar WN, Waxman SG: alpha-SNS produces the slow TTX-resistant sodium current in large cutaneous afferent DRG neurons. *J Neurophysiol* 2000, **84**:710–718.
23. Lai J, Gold MS, Kim CS, Bian D, Ossipov MH, Hunter JC, Porreca F: Inhibition of neuropathic pain by decreased expression of the tetrodotoxin-resistant sodium channel, Nav1.8. *Pain* 2002, **95**:143–152.
24. Fukuoka T, Kobayashi K, Yamanaka H, Obata K, Dai Y, Noguchi K: Comparative study of the distribution of the alpha-subunits of voltage-gated sodium channels in normal and axotomized rat dorsal root ganglion neurons. *J Comp Neurol* 2008, **510**:188–206.
25. Shields SD, Ahn HS, Yang Y, Han C, Seal RP, Wood JN, Waxman SG, Dib-Hajj SD: Nav1.8 expression is not restricted to nociceptors in mouse peripheral nervous system. *Pain* 2012, **153**(10):2017–2030.
26. Weiser T: Ambroxol: a CNS drug? *CNS Neurosci Ther* 2008, **14**:17–24.
27. Gaida W, Klinder K, Arndt K, Weiser T: Ambroxol, a Nav1.8-preferring Na(+) channel blocker, effectively suppresses pain symptoms in animal models of chronic, neuropathic and inflammatory pain. *Neuropharmacology* 2005, **49**:1220–1227.
28. Moon JY, Song S, Yoon SY, Roh DH, Kang SY, Park JH, Beitz AJ, Lee JH: The differential effect of intrathecal Nav1.8 blockers on the induction and maintenance of capsaicin- and peripheral ischemia-induced mechanical allodynia and thermal hyperalgesia. *Anesth Analg* 2012, **114**:215–223.
29. Weiser T, Wilson N: Inhibition of tetrodotoxin (TTX)-resistant and TTX-sensitive neuronal Na(+) channels by the secretolytic ambroxol. *Mol Pharmacol* 2002, **62**:433–438.
30. Tetreault P, Dansereau MA, Dore-Savard L, Beaudet N, Sarret P: Weight bearing evaluation in inflammatory, neuropathic and cancer chronic pain in freely moving rats. *Physiol Behav* 2011, **104**:495–502.
31. Sarret P, Esdaile MJ, Perron A, Martinez J, Stroth T, Beaudet A: Potent spinal analgesia elicited through stimulation of NTS2 neurotensin receptors. *J Neurosci* 2005, **25**:8188–8196.
32. Zhou Y, Li GD, Zhao ZQ: State-dependent phosphorylation of epsilon-isozyme of protein kinase C in adult rat dorsal root ganglia after inflammation and nerve injury. *J Neurochem* 2003, **85**:571–580.
33. McLean MJ, Bennett PB, Thomas RM: Subtypes of dorsal root ganglion neurons based on different inward currents as measured by whole-cell voltage clamp. *Mol Cell Biochem* 1988, **80**:95–107.

34. Cummins TR, Waxman SG: Downregulation of tetrodotoxin-resistant sodium currents and upregulation of a rapidly repriming tetrodotoxin-sensitive sodium current in small spinal sensory neurons after nerve injury. *J Neurosci* 1997, **17**:3503–3514.
35. Gold MS: Tetrodotoxin-resistant Na⁺ currents and inflammatory hyperalgesia. *Proc Natl Acad Sci USA* 1999, **96**:7645–7649.
36. Roy ML, Narahashi T: Differential properties of tetrodotoxin-sensitive and tetrodotoxin-resistant sodium channels in rat dorsal root ganglion neurons. *J Neurosci* 1992, **12**:2104–2111.
37. Cang CL, Zhang H, Zhang YQ, Zhao ZQ: PKCepsilon-dependent potentiation of TTX-resistant Nav1.8 current by neurokinin-1 receptor activation in rat dorsal root ganglion neurons. *Mol Pain* 2009, **5**:33.
38. Rush AM, Craner MJ, Kageyama T, Dib-Hajj SD, Waxman SG, Ranscht B: Contactin regulates the current density and axonal expression of tetrodotoxin-resistant but not tetrodotoxin-sensitive sodium channels in DRG neurons. *Eur J Neurosci* 2005, **22**:39–49.
39. Zhu YF, Henry JL: Excitability of Abeta sensory neurons is altered in an animal model of peripheral neuropathy. *BMC Neurosci* 2012, **13**:15.
40. Zhu YF, Wu Q, Henry JL: Changes in functional properties of A-type but not C-type sensory neurons in vivo in a rat model of peripheral neuropathy. *J Pain Res* 2012, **5**:175–192.
41. Wu Q, Henry JL: Changes in Abeta non-nociceptive primary sensory neurons in a rat model of osteoarthritis pain. *Mol Pain* 2010, **6**:37.
42. Song Y, Li HM, Xie RG, Yue ZF, Song XJ, Hu SJ, Xing JL: Evoked bursting in injured Abeta dorsal root ganglion neurons: a mechanism underlying tactile allodynia. *Pain* 2012, **153**:657–665.
43. Novakovic SD, Tzoumaka E, McGivern JG, Haraguchi M, Sangameswaran L, Gogas KR, Eglén RM, Hunter JC: Distribution of the tetrodotoxin-resistant sodium channel PN3 in rat sensory neurons in normal and neuropathic conditions. *J Neurosci* 1998, **18**:2174–2187.
44. Miao XR, Gao XF, Wu JX, Lu ZJ, Huang ZX, Li XQ, He C, Yu WF: Bilateral downregulation of Nav1.8 in dorsal root ganglia of rats with bone cancer pain induced by inoculation with Walker 256 breast tumor cells. *BMC Cancer* 2010, **10**:216.
45. Gould HJ 3rd, England JD, Liu ZP, Levinson SR: Rapid sodium channel augmentation in response to inflammation induced by complete Freund's adjuvant. *Brain Res* 1998, **802**:69–74.
46. Black JA, Liu S, Tanaka M, Cummins TR, Waxman SG: Changes in the expression of tetrodotoxin-sensitive sodium channels within dorsal root ganglia neurons in inflammatory pain. *Pain* 2004, **108**:237–247.
47. Gould HJ 3rd, England JD, Soignier RD, Nolan P, Minor LD, Liu ZP, Levinson SR, Paul D: Ibuprofen blocks changes in Na v 1.7 and 1.8 sodium channels associated with complete Freund's adjuvant-induced inflammation in rat. *J Pain* 2004, **5**:270–280.
48. Villarreal CF, Sachs D, Cunha FQ, Parada CA, Ferreira SH: The role of Na(V) 1.8 sodium channel in the maintenance of chronic inflammatory hypernociception. *Neurosci Lett* 2005, **386**:72–77.
49. Strickland IT, Martindale JC, Woodhams PL, Reeve AJ, Chessell IP, McQueen DS: Changes in the expression of Nav1.7, Nav1.8 and Nav1.9 in a distinct population of dorsal root ganglia innervating the rat knee joint in a model of chronic inflammatory joint pain. *Eur J Pain* 2008, **12**:564–572.
50. Coggeshall RE, Tate S, Carlton SM: Differential expression of tetrodotoxin-resistant sodium channels Nav1.8 and Nav1.9 in normal and inflamed rats. *Neurosci Lett* 2004, **355**:45–48.
51. Swanwick RS, Pristera A, Okuse K: The trafficking of Na(V)1.8. *Neurosci Lett* 2010, **486**:78–83.
52. Morgan JR, Gebhart GF: Characterization of a model of chronic orofacial hyperalgesia in the rat: contribution of NA(V) 1.8. *J Pain* 2008, **9**:522–531.
53. Gold MS, Weinreich D, Kim CS, Wang R, Treanor J, Porreca F, Lai J: Redistribution of Na(V)1.8 in uninjured axons enables neuropathic pain. *J Neurosci* 2003, **23**:158–166.
54. Thakor DK, Lin A, Matsuka Y, Meyer EM, Ruangsri S, Nishimura I, Spigelman I: Increased peripheral nerve excitability and local Nav1.8 mRNA up-regulation in painful neuropathy. *Mol Pain* 2009, **5**:14.
55. Yiangou Y, Birch R, Sangameswaran L, Eglén R, Anand P: SNS/PN3 and SNS2/NaN sodium channel-like immunoreactivity in human adult and neonate injured sensory nerves. *FEBS Lett* 2000, **467**:249–252.
56. Coward K, Plumpton C, Facer P, Birch R, Carlstedt T, Tate S, Bountra C, Anand P: Immunolocalization of SNS/PN3 and NaN/SNS2 sodium channels in human pain states. *Pain* 2000, **85**:41–50.
57. Kretschmer T, Happel LT, England JD, Nguyen DH, Tiel RL, Beuerman RW, Kline DG: Accumulation of PN1 and PN3 sodium channels in painful human neuroma—evidence from immunocytochemistry. *Acta Neurochir (Wien)* 2002, **144**:803–810. Discussion 810.
58. Bucknill AT, Coward K, Plumpton C, Tate S, Bountra C, Birch R, Sandison A, Hughes SP, Anand P: Nerve fibers in lumbar spine structures and injured spinal roots express the sensory neuron-specific sodium channels SNS/PN3 and NaN/SNS2. *Spine (Phila Pa 1976)* 2002, **27**:135–140.
59. Black JA, Nikolajsen L, Kroner K, Jensen TS, Waxman SG: Multiple sodium channel isoforms and mitogen-activated protein kinases are present in painful human neuromas. *Ann Neurol* 2008, **64**:644–653.
60. Ruangsri S, Lin A, Mulpuri Y, Lee K, Spigelman I, Nishimura I: Relationship of axonal voltage-gated sodium channel 1.8 (Nav1.8) mRNA accumulation to sciatic nerve injury-induced painful neuropathy in rats. *J Biol Chem* 2011, **286**:39836–39847.
61. England S, Bevan S, Docherty RJ: PGE2 modulates the tetrodotoxin-resistant sodium current in neonatal rat dorsal root ganglion neurons via the cyclic AMP-protein kinase A cascade. *J Physiol* 1996, **495**(Pt 2):429–440.
62. Rush AM, Waxman SG: PGE2 increases the tetrodotoxin-resistant Nav1.9 sodium current in mouse DRG neurons via G-proteins. *Brain Res* 2004, **1023**:264–271.
63. Joshi SK, Mikusa JP, Hernandez G, Baker S, Shieh CC, Neelands T, Zhang XF, Niforatos W, Kage K, Han P, Krafte D, Faltynek C, Sullivan JP, Jarvis MF, Honore P: Involvement of the TTX-resistant sodium channel Nav 1.8 in inflammatory and neuropathic, but not post-operative, pain states. *Pain* 2006, **123**:75–82.
64. Wang JG, Strong JA, Xie W, Zhang JM: Local inflammation in rat dorsal root ganglion alters excitability and ion currents in small-diameter sensory neurons. *Anesthesiology* 2007, **107**:322–332.
65. Bielefeldt K, Ozaki N, Gebhart GF: Mild gastritis alters voltage-sensitive sodium currents in gastric sensory neurons in rats. *Gastroenterology* 2002, **122**:752–761.
66. Almarestani L, Fitzcharles MA, Bennett GJ, Ribeiro-da-Silva A: Imaging studies in Freund's complete adjuvant model of regional polyarthritis, a model suitable for the study of pain mechanisms, in the rat. *Arthritis Rheum* 2011, **63**:1573–1581.
67. Atsey GP, Roberts JS, Paul D, Diamond I, Gould HJ 3rd: Ranolazine attenuation of CFA-induced mechanical hyperalgesia. *Pain Med* 2010, **11**:119–126.
68. Ekberg J, Jayamanne A, Vaughan CW, Aslan S, Thomas L, Mould J, Drinkwater R, Baker MD, Abrahamson B, Wood JN, Adams DJ, Christie MJ, Lewis RJ: muO-conotoxin MrVIB selectively blocks Nav1.8 sensory neuron specific sodium channels and chronic pain behavior without motor deficits. *Proc Natl Acad Sci USA* 2006, **103**:17030–17035.
69. Hillsley K, Lin JH, Stanis A, Grundy D, Aerssens J, Peeters PJ, Moechars D, Coulie B, Stead RH: Dissecting the role of sodium currents in visceral sensory neurons in a model of chronic hyperexcitability using Nav1.8 and Nav1.9 null mice. *J Physiol* 2006, **576**:257–267.
70. Jarvis MF, Honore P, Shieh CC, Chapman M, Joshi S, Zhang XF, Kort M, Carroll W, Marron B, Atkinson R, Thomas J, Liu D, Krambis M, Liu Y, McGaraughy S, Chu K, Roeloffs R, Zhong C, Mikusa JP, Hernandez G, Gauvin D, Wade C, Zhu C, Pai M, Scanio M, Shi L, Drizin I, Gregg R, Matulenko M, Hakeem A, et al: A-803467, a potent and selective Nav1.8 sodium channel blocker, attenuates neuropathic and inflammatory pain in the rat. *Proc Natl Acad Sci USA* 2007, **104**:8520–8525.
71. Kort ME, Drizin I, Gregg RJ, Scanio MJ, Shi L, Gross MF, Atkinson RN, Johnson MS, Pacofsky GJ, Thomas JB, Carroll WA, Krambis MJ, Liu D, Shieh CC, Zhang X, Hernandez G, Mikusa JP, Zhong C, Joshi S, Honore P, Roeloffs R, Marsh KC, Murray BP, Liu J, Werness S, Faltynek CR, Krafte DS, Jarvis MF, Chapman ML, Marron BE: Discovery and biological evaluation of 5-aryl-2-fururamides, potent and selective blockers of the Nav1.8 sodium channel with efficacy in models of neuropathic and inflammatory pain. *J Med Chem* 2008, **51**:407–416.
72. Laird JM, Souslova V, Wood JN, Cervero F: Deficits in visceral pain and referred hyperalgesia in Nav1.8 (SNS/PN3)-null mice. *J Neurosci* 2002, **22**:8352–8356.
73. Porreca F, Lai J, Bian D, Wegert S, Ossipov MH, Eglén RM, Kassotakis L, Novakovic S, Rabert DK, Sangameswaran L, Hunter JC: A comparison of the potential role of the tetrodotoxin-insensitive sodium channels, PN3/SNS and NaN/SNS2, in rat models of chronic pain. *Proc Natl Acad Sci USA* 1999, **96**:7640–7644.

74. Schuelert N, McDougall JJ: Involvement of Nav 1.8 sodium ion channels in the transduction of mechanical pain in a rodent model of osteoarthritis. *Arthritis Res Ther* 2012, **14**:R5.
75. Veneroni O, Maj R, Calabresi M, Faravelli L, Fariello RG, Salvati P: Anti-allodynic effect of NW-1029, a novel Na(+) channel blocker, in experimental animal models of inflammatory and neuropathic pain. *Pain* 2003, **102**:17–25.
76. Yu YQ, Zhao F, Guan SM, Chen J: Antisense-mediated knockdown of Na (V)1.8, but not Na(V)1.9, generates inhibitory effects on complete Freund's adjuvant-induced inflammatory pain in rat. *PLoS One* 2011, **6**:e19865.
77. Hama AT, Plum AW, Sagen J: Antinociceptive effect of ambroxol in rats with neuropathic spinal cord injury pain. *Pharmacol Biochem Behav* 2010, **97**:249–255.
78. Leffler A, Reckzeh J, Nau C: Block of sensory neuronal Na⁺ channels by the secretolytic ambroxol is associated with an interaction with local anesthetic binding sites. *Eur J Pharmacol* 2010, **630**:19–28.
79. Joshi SK, Honore P, Hernandez G, Schmidt R, Gomtsyan A, Scanio M, Kort M, Jarvis MF: Additive antinociceptive effects of the selective Nav1.8 blocker A-803467 and selective TRPV1 antagonists in rat inflammatory and neuropathic pain models. *J Pain* 2009, **10**:306–315.
80. McGaraughty S, Chu KL, Scanio MJ, Kort ME, Faltynek CR, Jarvis MF: A selective Nav1.8 sodium channel blocker, A-803467 [5-(4-chlorophenyl-N-(3,5-dimethoxyphenyl)furan-2-carboxamide)], attenuates spinal neuronal activity in neuropathic rats. *J Pharmacol Exp Ther* 2008, **324**:1204–1211.
81. Kohama I, Ishikawa K, Kocsis JD: Synaptic reorganization in the substantia gelatinosa after peripheral nerve neuroma formation: aberrant innervation of lamina II neurons by Abeta afferents. *J Neurosci* 2000, **20**:1538–1549.
82. Lekan HA, Carlton SM, Coggeshall RE: Sprouting of A beta fibers into lamina II of the rat dorsal horn in peripheral neuropathy. *Neurosci Lett* 1996, **208**:147–150.
83. Nakamura SI, Myers RR: Injury to dorsal root ganglia alters innervation of spinal cord dorsal horn lamina involved in nociception. *Spine (Phila Pa 1976)* 2000, **25**:537–542.
84. Okamoto M, Baba H, Goldstein PA, Higashi H, Shimoji K, Yoshimura M: Functional reorganization of sensory pathways in the rat spinal dorsal horn following peripheral nerve injury. *J Physiol* 2001, **532**:241–250.
85. Shortland P, Kinman E, Molander C: Sprouting of A-fibre primary afferents into lamina II in two rat models of neuropathic pain. *Eur J Pain* 1997, **1**:215–227.
86. Woolf CJ, Shortland P, Coggeshall RE: Peripheral nerve injury triggers central sprouting of myelinated afferents. *Nature* 1992, **355**:75–78.
87. Woolf CJ, Shortland P, Reynolds M, Ridings J, Doubell T, Coggeshall RE: Reorganization of central terminals of myelinated primary afferents in the rat dorsal horn following peripheral axotomy. *J Comp Neurol* 1995, **360**:121–134.
88. Liu CN, Michaelis M, Amir R, Devor M: Spinal nerve injury enhances subthreshold membrane potential oscillations in DRG neurons: relation to neuropathic pain. *J Neurophysiol* 2000, **84**:205–215.
89. Wall PD, Gutnick M: Ongoing activity in peripheral nerves: the physiology and pharmacology of impulses originating from a neuroma. *Exp Neurol* 1974, **43**:580–593.
90. Amir R, Devor M: Chemically mediated cross-excitation in rat dorsal root ganglia. *J Neurosci* 1996, **16**:4733–4741.
91. Devor M, Wall PD: Cross-excitation in dorsal root ganglia of nerve-injured and intact rats. *J Neurophysiol* 1990, **64**:1733–1746.
92. Utschneider D, Kocsis J, Devor M: Mutual excitation among dorsal root ganglion neurons in the rat. *Neurosci Lett* 1992, **146**:53–56.
93. Amir R, Devor M: Functional cross-excitation between afferent A- and C-neurons in dorsal root ganglia. *Neuroscience* 2000, **95**:189–195.

doi:10.1186/1742-2094-11-45

Cite this article as: Belkouch et al.: Functional up-regulation of Na_v1.8 sodium channel in A β afferent fibers subjected to chronic peripheral inflammation. *Journal of Neuroinflammation* 2014 **11**:45.

Submit your next manuscript to BioMed Central and take full advantage of:

- Convenient online submission
- Thorough peer review
- No space constraints or color figure charges
- Immediate publication on acceptance
- Inclusion in PubMed, CAS, Scopus and Google Scholar
- Research which is freely available for redistribution

Submit your manuscript at
www.biomedcentral.com/submit

